The scanning laser ophthalmoscope

1997 Phys. Med. Biol. 42 951

(http://iopscience.iop.org/0031-9155/42/5/014)

Phys. Med. Biol. **42** (1997) 951–966. Printed in the UK PII: S0031-9155(97)80692-6

The scanning laser ophthalmoscope

P F Sharp and A Manivannan

Department of Biomedical Physics and Bioengineering, University of Aberdeen and Aberdeen Royal Hospitals NHS Trust, Foresterhill, Aberdeen AB9 2ZD, UK

Received 6 December 1995

Abstract. The imaging of the fundus of the eye poses two major technical challenges. First, it is necessary for both the illuminating and reflected beams to pass through the same aperture, the iris. In some commonly used instruments this leads to the use of levels of illumination close to the maximum tolerable by a patient. Second, in order to visualize the different structures present in the various layers of the fundus it is necessary to perform tomographic imaging.

The scanning laser ophthalmoscope provides an answer to these particular problems. By scanning the fundus with a narrow laser beam most of the area of the iris is then available for the reflected light and so the intensity of the illuminating beam can be kept low, making it more acceptable for patients. The use of confocal imaging allows 3D images to be produced.

In this short review the performance of the instrument will be discussed and its application to a number of clinical problems in ophthalmology considered. Finally there will be a brief description of other instrumentation currently under development.

1. Imaging the fundus

The challenge of imaging the fundus is twofold. First, there is the problem of how to view the structure when there is only one aperture available through which both illumination and viewing beams must pass. Second, as the fundus consists of a number of distinct functional layers, it is important to be able to image tomographically. However, as the fundal thickness varies from 500 μm to about 2000 μm the imaging system must have high spatial resolution.

Imaging of the fundus is carried out either by direct or indirect ophthalmoscopy. In direct ophthalmoscopy the illuminated and reflected beams can be separated by various methods (Colenbrander 1980), such as a semi-reflecting mirror, a mirror with a central aperture or a prism. Unfortunately this gives a small field of view. In indirect ophthalmoscopy an ophthalmoscopic lens is used so as to increase the field of view while maintaining mutual correlation between the pupils and fundi, respectively of patient and observer.

The main instrument for recording images of the fundus is the fundus camera (Leutwein and Littmann 1985). This works on the principle of indirect ophthalmoscopy, except that the image can be recorded on photographic film. Recently the film has been replaced by a CCD camera which allows direct digital imaging to be performed (Shiraki *et al* 1991). However, the instrument is limited to planar imaging, and has non-uniform illumination.

2. The scanning laser ophthalmoscope (SLO)

Webb *et al* (1980) reported a method for imaging the retina using a laser; a detailed discussion of the principles of the confocal SLO is given by Webb *et al* (1987). Scanning

0031-9155/97/050951+16$19.50

devices use a different approach to imaging from the fundus camera. A highly collimated narrow beam of light from a laser is swept over the retina, delivering all its energy to a very small spot for a very short time. Light returned from that spot is detected and synchronously decoded to form an image on a monitor.

Several versions of the SLO have been constructed by various research groups (Webb *et al* 1987, Plesch *et al* 1987, Wynn-Williams and Crowe 1986, Van Norren and Van De Kraats 1989) and two commercial systems are currently available (Rodenstock and Zeiss). The SLO has been used for various routine clinical studies such as fluorescein angiography (Nasemann and Muller 1990, Scheider and Schroedel 1989) as well as in new exciting applications such as the quantification of retina blood flow parameters (Wolf *et al* 1990, Arend *et al* 1995a, b, Nishiwaki *et al* 1995, Kimura *et al* 1995, Khoobehi and Peyman 1994, Ohnishi *et al* 1994a), static fundus-controlled perimetry (Sturmer *et al* 1990), and three-dimensional optic disc topography (Burk *et al* 1990).

2.1. Principles of retinal illumination used in the SLO

The optics of the eye requires that illumination and observation of the retina be carried out through the same optical pathway. In conventional fundoscopy, a large area of post-equatorial retina is illuminated through the outer circumference of the dilated pupil, while a region of the total retina is observed through the central pupil (figure 1(a)). Here, within the limited area of pupil, the exit aperture is smaller than the entrance aperture. Unfortunately, this reduces the amount of detectable light by a factor of about 16 and so limits image quality (Plesch *et al* 1987).

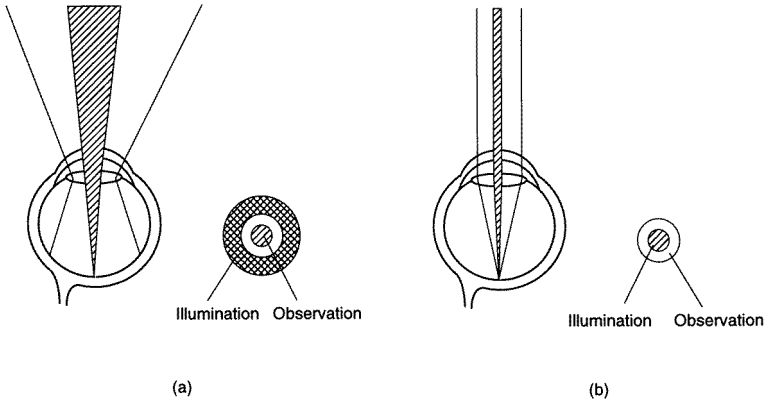

Figure 1. Illumination and observation of the retina by (a) the fundus camera and (b) the SLO.

The illumination and observation apertures of the fundus camera are inverted in the SLO, i.e., a small aperture is used for illumination and the remaining large area of the pupil is used for collection of light reflected from the retina (figure 1(b)). The optical collection efficiency is improved, allowing lower light intensity levels to be used.

2.2. The principle of operation of the SLO

The operating principle of the SLO has been explained in many papers (for example, Webb *et al* 1980, 1987, Plesch *et al* 1987, Webb 1990, Woon *et al* 1990, Manivannan *et al* 1993).

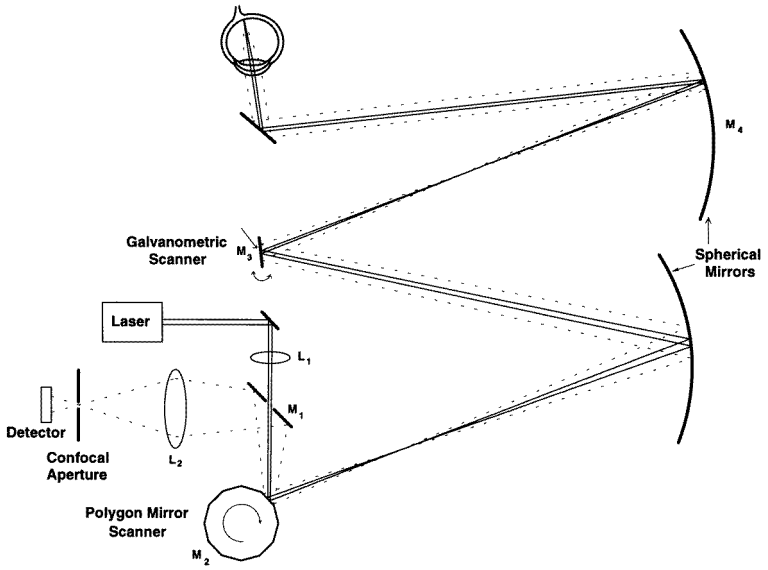

Figure 2. An optical diagram of the SLO.

A laser beam of 1 mm diameter is pre-shaped by a lens (L_1) so as to be in focus at the retina (figure 2). The beam passes through a 2 mm aperture (M_1) which is used as beam separator between the illuminating and reflected light. The laser beam is then deflected horizontally by a rotating polygon mirror (M_2), to form a line scan. The number of facets of the polygon determines the angle of deflection which, in turn, determines the angle scanned in the horizontal direction. A galvanometric mirror (M_3) deflects the beam vertically to form a two-dimensional raster. The two-dimensional raster is focused by a spherical mirror (M_4) to a single spot at the position of the patient's lens. The optics of the eye then focuses this on to the retina. The light reflected from the retina (dotted line in figure 2) emerges from a larger exit aperture, travels back along the same path as the illumination beam and is descanned by the two scanning mirrors. The light is collected by the beam separator and focused by a lens (L_2) onto a photodetector. The signal from the photodetector can then either be recorded on video-tape or fed to a frame-grabber interfaced to a computer.

2.3. Modes of operation

The SLO can be used in three different imaging modes; direct or non-confocal, confocal, and indirect (Manivannan *et al* 1993) (also known as the Tyndall (Webb *et al* 1987), dark-field (Woon *et al* 1990), or scatter mode). The mode of operation basically depends upon the size and position of the confocal aperture.

In the direct mode, the confocal aperture is very large compared to the size of the illumination spot. Light scattered from the point of illumination may undergo multiple reflections and escape through the iris of the eye. If the confocal aperture is large (e.g., 1 mm), this light may pass through it and reach the detector, so contributing to a reduction in contrast (figure 3). In the direct mode, the depth of focus is large (a few millimetres) and the overall brightness of the image is high as light from all layers of the retina and the choroid contributes to the image.

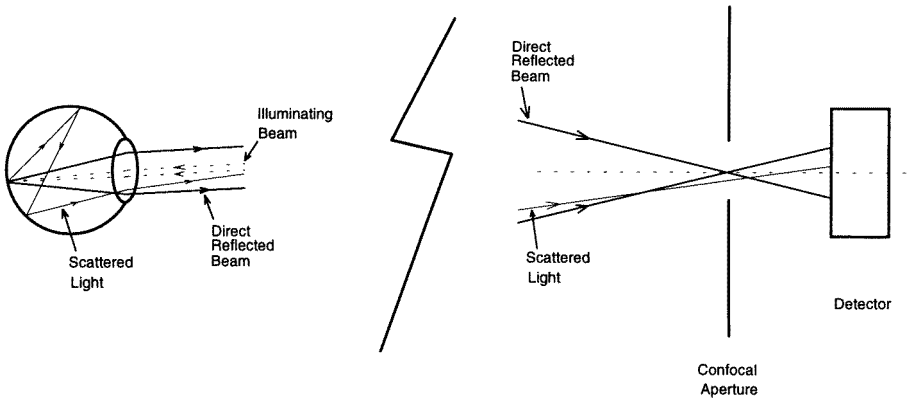

Figure 3. Imaging in the direct mode.

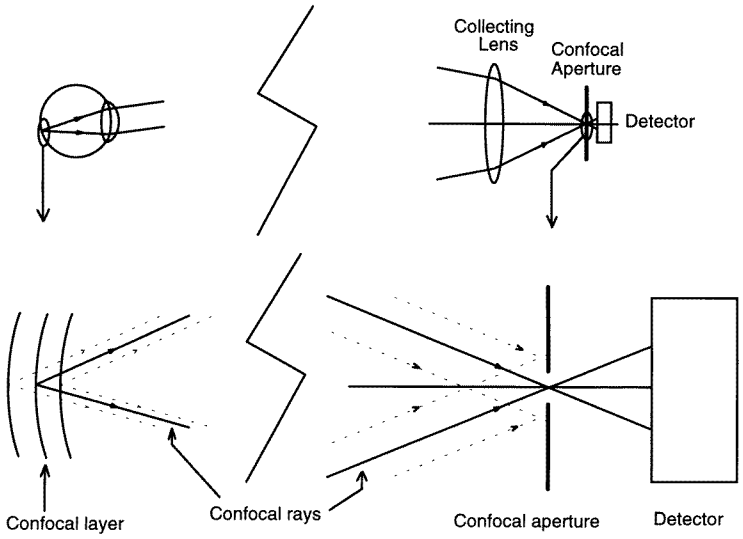

Figure 4. Principles of confocal imaging.

In the confocal mode, the aperture size is reduced, producing two advantages over the direct mode. First, light scattered from layers or areas other than the point of illumination are blocked by the confocal aperture. The second advantage is that the position of the confocal aperture determines from which layer in the fundus the reflected light is collected, so enabling tomographic imaging to be performed. The principle of tomographic imaging using the confocal aperture is demonstrated in figure 4. Three layers of the retina are shown in the figure. The rays from the confocal layer (solid lines) pass through the confocal aperture whereas the rays from either the layers above or below the confocal layer (dotted lines) are blocked by the confocal aperture.

Theoretical calculations show that light from layers that are 400 μm apart focus at confocal points that are 365 μm apart (Manivannan *et al* 1993). The depth of focus depends upon the aperture size. For example, with a 40 μm diameter confocal aperture,

the depth of focus is approximately 400 μm, this reduces to 100 μm for an aperture size of 10 μm. The effect of the confocal aperture on contrast can be seen in figure 5(A) and (B).

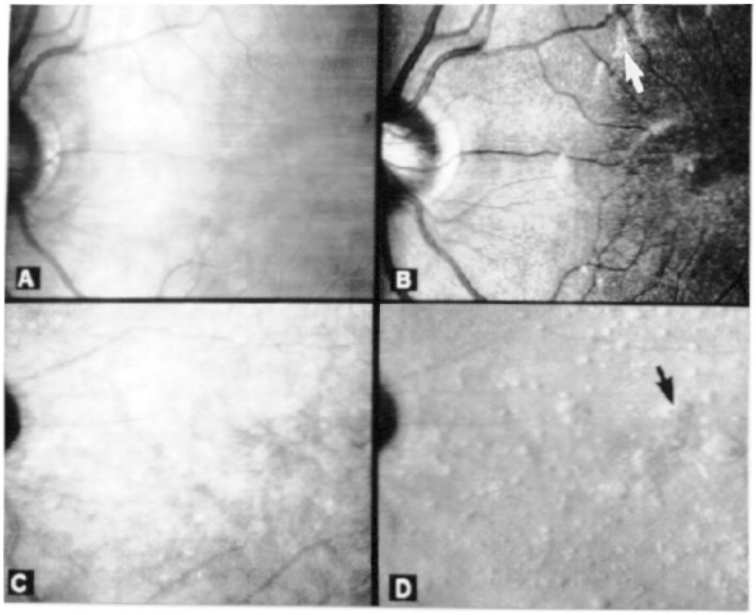

Figure 5. The images in figures 5(A) and (B) were captured from a normal volunteer. The image in figure 5(A) was recorded in the direct mode using a 1000 μm aperture and that in figure 5(B) in the confocal mode with a 100 μm one. The contrast has improved greatly with the confocal mode but the overall brightness of the image is reduced as less light is collected from a smaller slice of the retina. The reflection from the internal limiting membrane shows up in the confocal mode (white arrow) but is masked by the other reflecting surfaces in the direct mode. The images in figures 5(C) and (D) were captured from a patient with drusen. The confocal view (figure 5(C)) at the retinal surface shows no abnormality. The indirect image shows the presence of drusen (black arrow) with an elevated appearance.

By using a large aperture with a central stop (occluder), a new mode of imaging called the indirect mode allows a different image of the fundus to be formed (Webb *et al* 1987, Webb and Delori 1988). In this mode, the directly reflected light from the fundus is blocked by the central stop and only the scattered light is allowed through by the annulus ring (figure 6). If the light scattered around the point of illumination is further scattered by the neighbouring tissues and manages to escape through the iris, then it can contribute to the brightness of the image. The indirect mode has been found to be useful for imaging drusen (Van de Velde *et al* 1990, Manivannan *et al* 1993, Hartnett and Elsner 1996) small opaque hemispherical deposits from the pigment epithelium that form on the Bruch membrane (figure 5(C) and (D)).

2.4. Performance measurements

It is important to have a quantitative measure of the performance of the SLO, yet very few studies have been carried out (Fitzke *et al* 1991, Plesch and Klingbeil 1989, Manivannan *et al* 1994b). Since the SLO is designed to image the retina, it is necessary to make

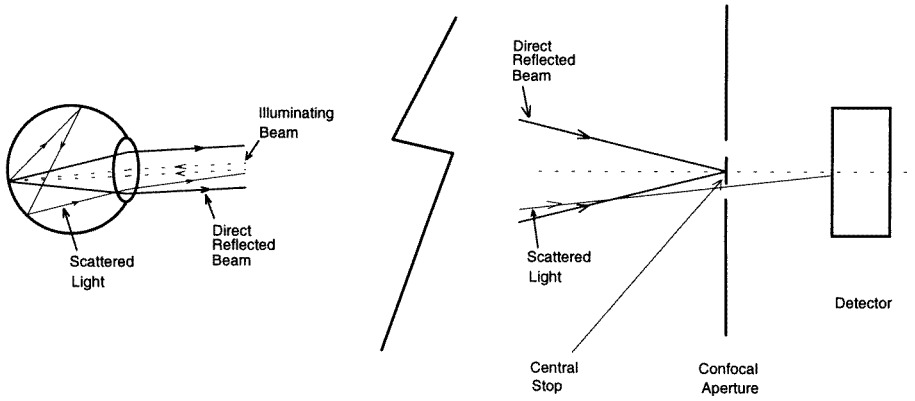

Figure 6. Imaging in the indirect mode.

measurements on test patterns as if they were situated on the retina. A simple approximation to the eye was used by Manivannan and colleagues (1994b), consisting of a 16 mm lens and a plane surface representing the fundus. The fundus was kept at a distance of 16 mm from the centre of the lens and a lens aperture of 5 mm was used. This was similar to the system used by Woon *et al* (1992).

The two most important performance characteristics are spatial resolution and slice thickness (axial or depth resolution). The spatial resolution of the SLO is determined by various factors such as wavelength, scan parameters, beam size at the cornea and the detector bandwidth, but ultimately is restricted by the spot size at the retina (Webb *et al* 1980). The eye's optics limits the spot size to about 10–20 μm (Webb 1990). The spatial resolution of imaging systems is often expressed in terms of the modulation transfer function, MTF. In the SLO the MTF will depend on the size, shape, and velocity of the scanning spot, the response characteristics of the detector, and the sampling rate of the digitizer.

Spatial resolution has been measured by two groups of researchers. Plesch and Klingbeil (1989) measured the MTF from the step response of the SLO to an 'appropriate target', which replaced the fundus of a phantom eye. The contrast was about 0.5 at 30 lines mm^{-1}, reducing to about 0.2 for 50 lines mm^{-1}. It was unclear whether the reported values are for the horizontal scanning or the vertical scanning. The authors also did not explain how they resolved a 10 μm line (50 lines mm^{-1}) with the 15 μm laser scanning spot. Manivannan *et al* (1994b) derived the MTF of a custom-made SLO from the image of an edge. A precision 'ronchi' ruling having horizontal and vertical sharp edges was used as the fundus of the model eye. The data was sampled every 8.5 μm in the horizontal direction and 10.0 μm in the vertical. The value of the MTF was about 0.5 at 15 lines mm^{-1} for the horizontal scanning and about 0.5 at 25 lines mm^{-1} for the vertical scanning.

The size of the confocal aperture will determine the 'slice' thickness from which light is collected. Reducing the size of the confocal aperture will result in a thinner slice within the limits imposed by the optics of the human eye (Campbell and Gubisch 1966, Dreher *et al* 1989). Depth resolution of 2600 μm for a 400 μm confocal aperture and 975 μm for a 100 μm confocal aperture was reported by Manivannan *et al* (1994b). A depth resolution of 300 μm has been reported by Plesch and Klingbeil (1989) with a 50 μm confocal aperture in the 20° field mode, using a phantom eye. Similar results have been reported by Woon *et al* (1992) using a 'confocal aperture 1' (size not reported) of a 'Rodenstock 101 cSLO' in the

20° field mode. A depth resolution of 300 μm was reported with a model eye consisting of a 16 mm lens and a micropositioner mounted mirror used as fundus. The depth resolution is finally limited by the numerical aperture of the human eye to approximately 150 μm (Plesch and Klingbeil 1989), but very narrow optical sections of 82 and 28 μm were reported using a 'micro-scanning attachment' (Fitzke *et al* 1991).

It is important to remember that reducing the confocal aperture size drastically reduces the light received by the SLO's photodetector. For example, using a 100 μm confocal aperture reduces the amount of light detected to 2% of that received with a 1000 μm aperture (Manivannan *et al* 1994b).

2.5. Safety

The potential hazards from the light levels used in ophthalmic instruments depends on the total light energy delivered to the patient's eye, exposure time, the size of the retinal area irradiated and the spectral distribution of the light source. While standards have been developed for the safe use of lasers (ANSI Z 136.1), the situation of intraoccular scanning is not considered (Plesch *et al* 1987). Klingbeil (1986) used thermal models to carry out an extensive study of the temperature rise for various conditions of intraoccular scanning and recommended maximum-permissible-exposure (MPE) levels for the safe use of SLOs. For a single-frame exposure of 26 ms, where each point on the retina is exposed for 75 ns, the maximum power that could be used was calculated to be 30 mW for a scanned area of 3.6 mm $\times$ 4.8 mm. For continuous exposure the power level should be reduced proportionately. For example, Plesch *et al* (1987) recommended an MPE of 6 mW for a duration of 100 s and Webb (1990) reported that the SLO could be safely used for as long as 1 h continuous viewing with power levels up to 100 μW. The SLO uses power levels very much lower than the other ophthalmic imaging devices and is thus considerably less hazardous than the conventional ophthalmoscopes.

3. Applications

3.1. Tomographic imaging of the fundus

Early detection of optic nerve head changes is important for the treatment of glaucoma. Recently various instruments have been developed to specifically investigate the status of the optic nerve head. The optic nerve head analyser from Rodenstock and the Humphrey retinal analyser use the stereoscopic imaging technique. Basically a set of stripes is projected onto the optic disc and stereoscopic images are captured (Shields *et al* 1987). The disparity between corresponding points of the stripes on the two images is used to calculate the relative depth. Optic disc parameters, such as cup/disc ratio, disc rim area, cup volume, disc elevation/depth, and total disc area, are measured.

The Heidelberg laser tomographic scanner uses the confocal technique to take images at 32 consecutive planes and the reflectance information from a particular point is used to develop topographic information (Kruse *et al* 1989). Recently, an improved version of this instrument has been introduced, known as the Heidelberg retinal tomograph (HRT).

Many papers have been published on the reproducibility and reliability of the technique (Kruse *et al* 1989, Dreher *et al* 1991, Rohrschneider *et al* 1993, Weinreb *et al* 1993, Janknecht and Funk 1994). Rohrschneider and colleagues made a detailed comparison of the published results and showed a large variation in reproducibility of rim area and cup volume measurements in normal eyes with a coefficient of variation varying from 4.6 to

17.7% and from 7.1 to 24.2% respectively. The cup volume of normals ranged from 0.007 to 1.98 mm^3 whereas for the glaucoma patients it varied from 0.192 to 2.579 mm^3. Due to large variation of various parameters of the optic disc, it seems unlikely that the technique will assist in the early diagnosis of glaucoma.

Stereoscopic imaging has been reported by Frambach *et al* (1993), who varied the position of the SLO so as to record right- and left-perspective images. These images were then viewed stereoscopically using either liquid crystal stereoscopic viewing goggles or a modified Allen separator. While this may aid the ophthalmologist in interpreting topographic features on the retinal surface, it is the ability to study the retina tomographically that perhaps offers the greatest clinical potential. Fitzke and Masters (1993) varied the ammetropia corrector lens of the SLO to acquire a series of images from the retinal surface down to the deep areas of the optic nerve head, each being separated by about 50 μm in depth. These images were then displayed using 3D volume rendering. A similar technique for acquiring a volume of data had been used by Bartsch *et al* (1989). The clinical value of this approach has yet to be evaluated.

3.2. Flow imaging

Fluorescein angiography (FAG) involves the intravenous administration of the fluorescein dye. Illuminating the eye with light of 488 nm wavelength and detecting the fluorescence, which occurs at a wavelength of 510 nm, through a barrier filter allows the flow of dye to be visualized. As the dye leaks from the choriocapillaris it is the retinal vessels that are visualized rather than the choroidal ones.

Wolf and colleagues (1990, 1991, 1993, 1994, Arend *et al* 1994a, Schulte *et al* 1996) used FAG to determine retinal haemodynamics. SLO fluorescein sequences were digitized from a video recording and curves generated to show the variation of fluorescence with time. From this information a number of parameters relating to retinal haemodynamics could be calculated. The macrocirculatory arm–retina time was measured as the time of first arrival of fluorescein in the superotemporal and inferotemporal arteries at a distance of 0.5 times the disc diameter from the disc margin. The mean arterial dye velocity was calculated from the time difference between the arrival at the previous points and at points two disc diameters from the disc margin along the same arteries. Finally, the arteriovenous passage time was defined as the difference between dye arrival times at the proximal reference point at the temporal arteries and an adjacent point at its corresponding vein. Reference values for normals have been published (Wolf *et al* 1994). In a comparison between normals and patients with open-angle glaucoma they found that arm–retina time did not differ, while in the glaucoma group the arteriovenous time was increased and mean dye velocity decreased.

They also described the visualization of fluorescent blobs (Wolf *et al* 1994); the hypofluorescent areas between the blobs they attribute to segments of cell-free plasma. This had originally been studied by Tanaka *et al* (1991) who reported the presence of fluorescent dots in 48% of patients imaged. By microscopic examination of blood samples mixed with fluorescein, they observed that leukocytes and platelets fluoresced, while erythrocytes did not. By measuring the distance moved by a dot between successive angiographic frames the velocity in the perifoveal capillaries could be calculated. This was found to be 1.2 mm s^{-1}; measurements on the hypofluorescent areas by Wolf gave an average velocity of 2.89 ± 0.41 mm s^{-1}. There is a debate as to whether flow should be measured using the fluorescent or hypofluorescent areas (Arend *et al* 1994b, Ohnishi *et al* 1994b).

Arend and colleagues (1995b) showed that, by monitoring the movement of the hypofluorescent areas, capillary flow in diabetics was significantly lower than that seen

in healthy subjects. Ohnishi *et al* (1994a) studied capillary blood flow in a patient with macular oedema. They found that the blood flow velocity in a juxta-foveolar capillary, measured by tracking the hyperfluorescent areas, was slowest (0.82 ± 0.13 mm s^{-1}) when the oedema was worst and improved (1.65 ± 0.17 mm s^{-1}) with the resolution of the oedema.

Unlike fluorescein, which leaks rapidly from the fenestrated choriocapillaris producing a diffuse background fluorescence, obscuring visualization of the deep choroidal vessels, indocyanine green (ICG) binds to protein in blood. It can, therefore, be used for fluorescence angiography of the choroidal system located deep in the fundus. Also, since it uses near-infrared light the absorption by the pigment epithelium and macular xanthophyll is relatively low. Unfortunately, because of its low fluorescence (4%) it was only with the introduction of the SLO that sufficiently good image quality could be achieved, although modified fundus cameras can now be used. The first results were reported by Scheider and Schroedel (1989) using a 780 nm exciting laser and a 820 nm barrier filter with an infra-red sensitive solid state detector. Scheider and colleagues demonstrated the clinical potential of the technique in a study of subretinal neovascular membranes (1992) and central serous choroidopathy (1993). Recently, Bischoff and colleagues (1995) have performed FAG and ICG angiography simultaneously by employing a selectively transmissible mirror to direct the different emitted wavelengths to separate detectors for the FAG and ICG angiography.

Simultaneous FAG and ICG angiography, albeit achieved by switching between exciter lasers and barrier filters, has been proposed by Maruyama *et al* (1995) for angiography of the iris. It was found that the fluorescence from the fluorescein was mostly blocked by iris pigment, while that from the ICG angiography at the infrared wavelength escaped such a fate.

Khoobehi and Peyman (1994) encapsulated fluorescein in liposomes, 0.1–2 μm in diameter. In FAG the liposomes appear as bright fluorescing spots against a largely dark background and can readily be recorded travelling through the retinal vessels. Blood velocity can be calculated from a video recording of the angiogram by measuring the distance travelled by a spot in a given time. One of the major advantages of the technique is that, as the contrast of the liposomes is so high, flow can be measured even in capillaries of a diameter much smaller than the spatial resolution of the SLO. Recently the same group have used ICG encapsulated in liposomes to study the choroidal circulation in primates (Peyman *et al* 1996a, b).

3.3. Autofluorescence

The fundus is autofluorescent; when illuminated by light in the range 450–500 nm, emissions with a peak between 550 and 600 nm are observed. This fluorescence is mainly due to the presence of a chromophore known as lipofuscin. Lipofuscin is found in the retinal pigmented epithelium (RPE) and is thought to reflect the metabolic activity that is determined largely by the rate of turnover of the outer segments of the photoreceptors. Measuring this fluorescence may provide a means for monitoring the metabolic activity associated with the photoreceptors. Von Ruckmann and colleagues (1995) produced images from this autofluorescence by using an SLO with illumination at 488 nm and detection through a barrier filter with low-frequency cut-off of 521 nm.

3.4. Use of different wavelengths

The optics of the human eye transmits wavelengths from 400 to 1000 nm enabling imaging to be carried out with a range of different wavelengths. Commercial SLOs often use argon

(488 and 514 nm), dye (500–620 nm), He–Ne (594 and 633 nm), or diode (670, 780, 805, and 830 nm) lasers. Lower wavelengths, such as argon, are mainly used to image the optic nerve head as this layer is highly reflective at this particular wavelength. The He–Ne laser gives a good image of the fundus, arteries and veins appearing with different contrasts, reflecting the difference in blood oxygenation. Near-infrared wavelengths are useful for imaging the deeper layers such as the choroid. Manivannan and colleagues (1994a; Kirkpatrick *et al* 1995) demonstrated that, by using infrared light, fundus images could be produced even in the presence of nuclear lens opacities. Quantitative reflectometry using various wavelengths was reported by Elsner *et al* (1990). The use of a specific wavelength to highlight a particular pathological condition is demonstrated in figure 7, which is of a patient with diabetic retinopathy.

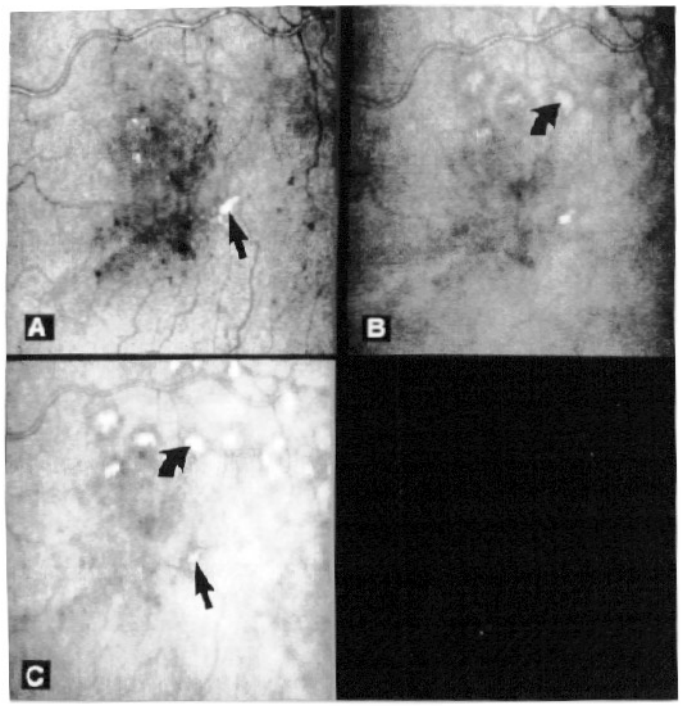

Figure 7. Figure 7(A), taken at 590 nm, shows the exudate as a highly reflective object (arrow) and the haemorrhages and microaneurysms as dark spots. In figure 7(B), taken at 670 nm, it can be seen that the exudate starts to lose its contrast with respect to the background. The patient had a laser treatment in the previous visit and the laser scars due to photocoagulation start to show up (curved arrow). Figure 7(C), taken at 780 nm, shows the laser scars very clearly (curved arrow) whereas the exudate is barely visible (arrow).

Since changes in the premacular vitreous appear to correlate with macular changes, the imaging of the posterior vitreous may prove a useful clinical tool. The large depth of focus available with the SLO makes it particularly useful in this situation. Kakehashi *et al* (1995) found an argon blue laser to be the best choice. The low penetration of the short-wavelength illumination has also been employed by Ogura and Honda (1993) to study abnormalities of the vitreo-retinal interface, in this case the presence of epiretinal membranes. The short-wavelength light is clearly reflected by the membrane, while switching to infrared

illumination allows the retina and choroid under the membrane to be examined. Staurenghi *et al* (1996) used infrared light to detect neovascular membranes.

3.5. Image processing

Many fundus diseases have visible pathological features that allow the disease to be readily identified. By employing image processing techniques the spatial extent of these features can be quantified so that the natural progression and response to various forms of treatment, such as laser therapy, can be reliably monitored. We have already developed computer techniques for the detection and quantification of diabetic macular oedema (Phillips *et al* 1990, 1991a), exudates (Phillips *et al* 1991b, 1993), and microaneurysms (Spencer *et al* 1992). This work is based on digitizing previously acquired retinal photographs and fluorescein angiograms taken with a fundus camera. The SLO has the advantage that it gives direct digital images of the fundus. Also, since the light beam is scanned over the fundus the illumination is uniform, so avoiding the need for shade correction (Spencer *et al* 1992, 1996). In situations where the dynamics of fluorescein flow are to be studied (subsection 3.2) the SLO can capture images at up to 25 frames s^{-1}, while the fundus camera is limited to about 1 s^{-1} due to the slow recharging time of its flash unit.

In a study involving imaging of patients with cataract, the quality of the SLO images appeared to be superior both to indirect ophthalmoscopy and fundus photography (Kirkpatrick *et al* 1995). Quantitative analysis of contrast of retinal vessels using image processing techniques demonstrated significantly higher contrast for the SLO images compared with digitized fundus photographs at all wavelengths tested (590, 670, and 780 nm) with the highest contrast being at 590 nm using the confocal mode.

3.6. Densitometry

Retinal densitometry is a technique for assessing the amount of photopigment in the retina, by measuring the amount of light reflected from the retina. By making one measurement with the eye dark adapted and a second after it has been exposed to bright light, it should be possible to distinguish areas in which the photoreceptors are abnormal. As such measurements may easily be confounded by the presence of scattered light, particularly from the anterior segment and vitreous, the use of confocal imaging with the SLO minimizes the problem. Van Norren and Van de Kraats (1989) and Cooper and colleagues (1992) have demonstrated the feasibility of the technique and claimed an accuracy comparable to that found with other equipment. A review of clinical applications is given by Liem *et al* (1996), but to date no clinical results have been published.

3.7. Retinal function testing

In planning the treatment of discrete areas of the retina by photocoagulation it is important to know which regions exhibit visual deficits. The presence of visual function is achieved by moving a stimulus over the retina and asking the patient whether or not it is visible. Timberlake and colleagues (1982) were the first to demonstrate how this could be achieved with the SLO. By using the imaging laser to produce the test stimulus it is possible to see the spatial location of the stimulus superimposed on the fundus image simultaneously with recording the patient's response. An acousto-optic modulator connected to a computer makes it possible to generate patterns in the illuminating beam by modulating its intensity (Timberlake *et al* 1989), such as the Snellen E stimulus for visual acuity, or black dots for

perimetry. The technique has been used to study the degree of loss of function associated with small holes and cysts in the retina (Acosta *et al* 1991, Sjaarda *et al* 1993a) macular atrophy (Sunness *et al* 1995), the effect of surgery (Sjaarda *et al* 1993b, Hudson *et al* 1995) and for evoking peripheral pattern electroretinograms (Horn *et al* 1996).

4. Other techniques

Ultimately, the performance of optical techniques will be limited by the optics of the eye; in-plane spatial resolution being limited to about 10 μm, while the best achievable slice thickness is about 600 μm (see subsection 2.3).

Higher axial resolution has been achieved by employing the technique of optical coherence tomography (OCT). The eye is illuminated using a coherent light source from either a laser or superluminescent diode. By employing interferometric techniques (low-coherence tomography) the depth of penetration of the reflected signal can be measured, while a beam scanning mechanism permits images to be made (Huang *et al* 1991, Hee *et al* 1995a, b, Puliafito *et al* 1995). The system is based around a Michelson interferometer in which low-coherence light from a superluminescent diode at 843 nm is used. The light is divided at a fibre coupler into reference and sample paths. Light reflected from a variable-distance reference mirror is recombined in the coupler with that back-scattered from the patient's eye. Temporal information is contained in the interference signal between the reference and sample beams, which is detected by a photodiode. A longitudinal profile of reflectivity versus depth into the fundus is obtained by translating the reference mirror while synchronously recording the magnitude of the resulting interference signal. The superluminescent diode has a coherence length of 10 μm and this defines the axial resolution of the system. The lateral resolution is 13 μm. To obtain a 3D image a sequence of longitudinal profiles is collected by scanning the probe beam across the retina while translating the reference mirror. A single scan line, consisting of 100 depth measurements, takes 2.5 s.

In OCT longitudinal motion between the eye and the measuring instrument will affect the depth measurement. To overcome this Drexler and colleagues (1995) have developed a dual-beam version of the technique, known as partial coherence tomography (PCT).

The depth resolution from OCT and PCT is the best achievable with any current imaging system; the retinal nerve fibre layer, choriocapillaris, and RPE layer are clearly visible as highly reflecting layers. The system has been used to study a variety of macular diseases including macular holes, oedema, exudates, and detachment of the retina and RPE (Puliafito *et al* 1995). It may also be useful in measuring the changes in retinal thickness that accompany many retinal diseases (Drexler *et al* 1995) and in measuring nerve fibre layer thickness (Schuman *et al* 1995).

The mechanism of imaging by OCT and PCT is dependent on strong reflection from different boundaries within the fundus and so is of particular value in those disease processes in which tissue interfaces are prominent. The two techniques do, however, suffer from a number of problems. As is also the case in ultrasound imaging, deeper structures can be masked by superficially located highly reflecting objects, such as hard exudates. Multiple scattering will also reduce image quality. The time to produce a full 3D scan is very long, of the order of 3–4 min and steps need to be taken to align shifts in scan lines produced by eye movements. Lateral resolution may also be affected by microsaccades, giving a lateral resolution of 150 μm.

The retinal nerve fibre layer (RNFL) consists of ganglion cell axons comprising parallel microtubules of diameter less than the wavelength of light. As such the RNFL should

behave as a birefringent medium and the polarization of the laser will, therefore, be retarded in its passage through this layer. The phase difference between the incident beam and the reflected one is reported as being linearly related to the RNFL thickness (Dreher *et al* 1992). While this technique allows relative, but not absolute, thickness to be measured, it raises the possibility of providing early detection of glaucomatous changes. Such measurements have been made by incorporating a polarization modulator and detector into the SLO. A good review of the technique is given by Tuulonen and Airaksinen (1996) but to date there is no clear evidence of its clinical value (Weinreb *et al* 1995).

Acknowledgments

The authors wish to acknowledge the financial support of Scotia Pharmaceuticals, the Wellcome Trust and the Scottish Office. Invaluable comments were received from Professor J Forrester, Dr J Olson, Dr K McHardy, Dr N Kirkpatrick, and Mr P Viera. The photographic assistance of Mr R Hutcheon is gratefully acknowledged.

References

Acosta F, Lashkari K, Reynaud X, Jalkh A E, van de Velde F and Chedid N 1991 Characterization of functional changes in macular holes and cysts *Ophthalmology* **98** 1820–3

Arend O, Harris A, Martin B J, Holin M and Wolf S 1994a Retinal blood velocities during carbogen breathing using scanning laser ophthalmoscopy *Acta Ophthalmol.* **72** 332–6

Arend O, Harris A, Sponsel W E, Remky A, Reim M, and Wolf S 1995a Macular capillary particle velocities: a blue field and scanning laser comparison *Grafes Arch. Clin. Exp. Ophthalmol.* **233** 244–9

Arend O, Harris A and Wolf S 1994b Capillary blood flow velocity measurements in cystoid macular edema with the scanning laser ophthalmoscope *Am. J. Ophthalmol.* **117** 819–20

Arend O, Wolf S, Harris A and Reim M 1995b The relationship of macular microcirculation to visual acuity in diabetic patients *Arch. Ophthalmol.* **113** 610–14

Bartsch D-U, Intaglietta M, Bille J F, Dreher A W, Gharib M and Freeman W R 1989 Confocal laser tomographic analysis of the retina in eyes with macular hole formation and other focal macular diseases *Am. J. Ophthalmol.* **108** 277–87

Bischoff P M, Niederberger H J, Torok B and Speiser P 1995 Simultaneous indocyanine green and fluorescein angiography *Retina* **15** 91–9

Burk R O W, Rohrschneider K, Volcker H E and Zinser G 1990 Analysis of three-dimensional optic disk topography by laser scanning tomography *Scanning Laser Ophthalmoscopy and Tomography* ed J E Nasemann and R O W Burk (Munich: Quintessenz) pp 161–76

Campbell F W and Gubisch R W 1966 Optical quality of the human eye *J. Physiol.* **186** 558–78

Colenbrander A 1980 Principles of ophthalmoscopy *Refraction and Clinical Optics* ed A Safir (Hagerstown: Harper and Row) ch 25, pp 475–95

Cooper R L, Eikelboom R H and Barry C J 1992 Correlations between densitometry of red-free photographs and reflectometry with the scanning laser ophthalmoscope in normal subjects and glaucoma patients *Int. Ophthalmol.* **16** 243–6

Dreher A W, Bille J F and Weinreb R N 1989 Active optical depth resolution improvement of the laser tomographic scanner *Appl. Opt.* **28** 804–8

Dreher A W, Reiter K and Weinreb R N 1992 Spatially resolved birefringence of the retinal nerve fiber layer assessed with a retinal laser ellipsometer *Appl. Optics.* **31** 3730–5

Dreher A W, Tso P C and Weinreb R N 1991 Reproducibility of topographic measurements of the normal and glaucomatous optic nerve head with the laser tomographic scanner *Am. J. Ophthalmol.* **111** 221–9

Drexler W, Hitzenberg C K, Sattmann H and Fercher A F 1995 Measurement of the thickness of fundus layers by partial coherence tomography *Opt. Eng* **34** 701–10

Elsner A E, Burns S A, Delori F C and Webb R H 1990 Quantitative reflectometry with the SLO *Scanning Laser Ophthalmoscopy and Tomography* ed J E Nasemann and R O W Burk (Munich: Quintessenz) pp 109–21

Fitzke F W and Masters B R 1993 Three-dimensional visualization of confocal sections of in vivo human fundus and optic nerve *Current Eye Res.* **12** 1015–18

Fitzke F W, Woon H, Timberlake G, Robinson L, Marshall J and Bird A C 1991 Optical modifications to a scanning laser ophthalmoscope for high magnification, narrow optical section imaging *Laser Light Ophthalmol.* **4** 7–14

Frambach D A, Dacey M P and Sadun A 1993 Stereoscopic photography with a scanning laser ophthalmoscope *Am. J. Ophthalmol.* **116** 484–8

Hartnett M E and Elsner A E 1996 Characteristics of exudative age-related macular degeneration determined *in vivo* with confocal and indirect infrared imaging *Opthalmology* **103** 58–71

Hee M R, Izatt J A, Swanson E A, Huang D, Schuman J S, Lin C P, Puliafito C A and Fujimoto J G 1995a Optical coherence tomography of the human retina *Arch. Ophthalmol.* **113** 325–32

Hee M R, Puliafito C A, Wong C, Duker J S, Reichel E, Schuman J S, Swanson E A, Fujimoto J G 1995b Optical coherence tomography of macular holes *Ophthalmology* **102** 748–56

Horn F, Mardin C, Korth M and Martus P 1996 Quadrant pattern ERG with SLO stimulation in normals and glaucoma patients *Grafes Arch. Clin. Exp. Ophthalmol.* **234** S174–9

Huang D, Swanson E A, Lin C P, Schuman J S, Stinson W G, Chang W, Hee M R, Flotte T, Gregory K, Pulafito C A and Fujimoto J G 1991 Optical coherence tomography *Science* **254** 1178–81

Hudson H L, Frambach D A and Lopez P F 1995 Relation of the functional and structural fundus changes after submacular surgery for neovascular age-related macular degeneration. *Br. J. Ophthalmol.* **79** 417–23

Janknecht P and Funk J 1994 Optic nerve head analyser and Heidelberg retina tomograph: accuracy and reproducibility of topographic measurements in a model eye and in volunteers. *Br. J. Ophthalmol.* **78** 760–8

Kakehashi A, Ishiko S, Konno S, Akiba J, Kado M and Yoshida A 1995 Observing the posterior vitreous by means of the scanning laser ophthalmoscope *Arch. Ophthalmol.* **113** 558–60

Khoobehi B and Peyman G A 1994 Fluorescent vesicle system. A new technique for measuring blood flow in the retina *Ophthalmology* **101** 1716–26

Kimura H, Kiryu J, Nishiwaki H, and Ogura Y 1995 A new fluorescent imaging procedure in vivo for evaluation of the retinal microcirculation in rats. *Current Eye Res.* **14** 223–8

Kirkpatrick J N P, Manivannan A, Gupta A K, Hipwell J, Forrester J V and Sharp P F 1995 Fundus imaging in patients with cataract: role for a variable wavelength scanning laser ophthalmoscope *Br. J. Ophthalmol.* **79** 892–9

Klingbeil U 1986 Safety aspects of laser scanning ophthalmoscopes *Health Phys.* **51** 81–93

Kruse F E, Burk R O, Volcker H E, Zinser G and Harbarth U 1989 Reproducibility of topographic measurements of the optic nerve head with laser tomographic scanning *Ophthalmology* **96** 1320–24

Leutwein K and Littmann H 1985 Fundus camera *Clinical Ophthalmology* vol 1, ed T D Duane (Philadelphia, PA: Harper and Row) ch 73

Leim A T A, Keunen J E E and van Norren D 1996 Clinical applications of fundus reflection densitometry *Surv. Ophthalmol.* **41** 37–50

Manivannan A, Kirkpatrick J N P, Sharp P F and Forrester J V 1994a Clinical investigation of an infrared digital scanning laser ophthalmoscope *Br. J. Ophthalmol.* **78** 84–90

Manivannan A, Sharp P F, and Forrester J V 1994b Performance measurements of an infrared digital scanning laser ophthalmoscope *Physiol. Meas.* **15** 317–24

Manivannan A, Sharp P F, Phillips R P and Forrester J V 1993 Digital fundus imaging using a scanning laser ophthalmoscope *Physiol. Meas.* **14** 43–56

Maruyama Y, Kishi S, Kamei Y, Shimizu R and Kimura Y 1995 Infrared angiography of the anterior ocular segment *Surv. Ophthalmol.* **39** S40–8

Nasemann J E and Muller M 1990 Scanning laser angiography *Scanning Laser Ophthalmoscopy and Tomography* ed J E Nasemann and R O W Burk (Munich: Quintessenz) pp 63–80

Nishiwaki H, Ogura Y, Kimura H, Kiryu J, and Honda Y 1995 Quantitative evaluation of leukocyte dynamics in retinal microcirculation *Invest. Ophthalmol. Vis. Sci.* **36** 123–30

Ogura Y and Honda Y 1993 Evaluation of idiopathic epiretinal membranes by a scanning laser ophthalmoscope *Br. J. Ophthalmol.* **77** 534–5

Ohnishi Y, Fujisawa K, Ishibashi, T and Kojima H 1994a Capillary blood flow velocity measurements in cystoid macular edema with the scanning laser ophthalmoscope *Am. J. Ophthalmol.* **117** 24–9

——1994b Capillary blood flow velocity measurements in cystoid macular edema with the scanning laser ophthalmoscope. Reply *Am. J. Ophthalmol.* **117** 820

Peyman G A, Khoobehi B, Shaibani S, Shamsnia S and Ribeiro I 1996a A fluorescent vesicle system for the measurement of blood velocity in the choroidal vessels *Ophthalmic Surg. Lasers* **27** 459–66

Peyman G A, Moshfeghi D M, Moshfeghi A A and Khoobehi B 1996b Fluorescent vesicle angiography with sodium fluorescein and indocyanine green *Ophthalmic Surg. Lasers* **27** 279–84

Phillips R P, Forrester J V and Sharp P F 1993 Automated detection and quantification of retinal exudates *Grafes Arch. Clin. Exp. Ophthalmol.* **231** 90–4

Phillips R P, Ross P G B, Sharp P F and Forrester J V 1990 Use of temporal information to quantify vascular leakage in fluorescein angiography of the retina *Clin. Phys. Physiol. Meas.* **11** (Supplement A) 81–5

Phillips R P, Ross P G, Tyska M, Sharp P F and Forrester J V 1991a Detection and quantification of hyperfluorescent leakage by computer analysis of fundus fluorescein angiograms *Grafes Arch. Clin. Exp. Ophthalmol.* **229** 329–35

Phillips R P, Spencer T, Ross P G B, Sharp P F and Forrester J V 1991b Quantification of diabetic maculopathy by digital imaging of the fundus *Eye* **5** 130–7

Plesch A and Klingbeil U 1989 *Optical Characteristics of a Scanning Laser Ophthalmoscope, SPIE* vol 1161 (Bellingham, WA: SPIE) pp 390–8

Plesch A, Klingbeil U and Bille J 1987 Digital laser scanning fundus camera *Appl. Opt.* **26** 1480–6

Puliafito C A, Hee M R, Lin C P, Reichel E, Schuman J S, Duker J S, Izatt J A, Swanson E A and Fujimoto J G 1995 Imaging of macular diseases with optical coherence tomography *Ophthalmology* **102** 217–29

Rohrschneider K, Burk R O and Volcker H E 1993 Reproducibility of topometric data acquisition in normal and glaucomatous optic nerve heads with the laser tomographic scanner *Grafes Arch. Clin. Exp. Ophthalmol.* **231** 457–64

Scheider A, Kaboth A and Neuhauser L 1992 Detection of subretinal neovascular membranes with indocyanine green and an infrared scanning laser ophthalmoscope *Am. J. Ophthalmol.* **113** 45–51

Scheider A, Nasemann J E and Lund O-E 1993 Fluorescein and indocyanine green angiographies of central serous choroidopathy by scanning laser ophthalmoscopy *Am. J. Ophthalmol.* **115** 50–6

Scheider A and Schroedel C 1989 High resolution indocyanine green angiography with a scanning laser ophthalmoscope *Am. J. Ophthalmol.* **108** 458–9

Schulte K, Wolf S, Arend O, Harris A, Henle C and Reim M 1996 Retinal haemodynamics during increased intraocular pressure *German J. Ophthalmol.* **5** 1–5

Schuman J S, Hee M R, Puliafito C A, Wong C, Pedut-Kloizman T, Lin C P, Hertzmark E, Izatt J A, Swanson E A and Fujimoto J G 1995 Quantification of nerve fibre layer thickness in normal and glaucomatous eyes using optical coherence tomography *Arch. Ophthalmol.* **113** 586–96

Shields M B, Martone J F, Shelton A R, Ollie A R and MacMillan J 1987 Reproducibility of topographic measurements with the optic nerve head analyzer. *Am. J. Ophthalmol.* **104** 581–6

Shiraki K, Harimura Y, Moriwaki M and Miki T 1991 Digital fluorescein fundus angiography with DFC-512 and IMAGEnet systems. *Eur. J. Ophthalmol.* **1** 39–44

Sjaarda R N, Frank D A, Glaser B M, Thompson J T and Murphy R P 1993a Assessment of vision in idiopathic macular holes with macular microperimetry using the scanning laser ophthalmoscope *Ophthalmology* **100** 1513–8

——1993b Resolution of absolute scotoma and improvement of relative scotomata after successful macular hole surgery *Am. J. Ophthalmol.* **116** 129–39

Spencer T, Olson J A, McHardy K, Sharp P F and Forrester J V 1996 An image-processing strategy for the segmentation and quantification of microaneurysms in fluorescein angiograms of the ocular fundus *Computers Biomed. Res.* **29** 284–302

Spencer T, Phillips R P, Sharp P F and Forrester J V 1992 Automated detection and quantification of microaneurysms in fluorescein angiograms *Grafes Arch. Clin. Exp. Ophthalmol.* **230** 36–41

Staurenghi G, Aschero M, Lacapria A, Gonnella P and Orzalesi N 1996 Visualization of neovascular membranes with infrared light without dye injection by means of a scanning laser ophthalmoscope *Arch. Ophthalmol.* **114** 365

Sturmer J, Schrodel C and Rappl W 1990 Scanning laser ophthalmoscope for static fundus-controlled perimetry *Scanning Laser Ophthalmoscopy and Tomography* ed J E Nasemann and R O W Burk (Munich: Quintessenz) pp 133–46

Sunness J A, Bressler N M and Maguire M G 1995 Scanning laser ophthalmoscopic analysis of the pattern of visual loss in age-related geographic atrophy of the macula *Am. J. Ophthalmol.* **119** 143–51

Tanaka T, Muraoka K and Shimizu K 1991 Fluorescein fundus angiography with scanning laser ophthalmoscope. Visibility of leukocytes and platelets in perifoveal capillaries *Ophthalmology* **98** 1824–9

Timberlake G T, Mainster M A, Webb R H, Hughes G W and Trempe C L 1982 Retinal localization of scotomata by scanning laser ophthalmoscopy *Invest. Ophthalmol. Vis. Sci.* **22** 91–7

Timberlake G T, Van de Velde F J and Jalkh A E 1989 Clinical use of scanning laser ophthalmoscope retinal function maps in macular disease *Lasers Light Ophthalmol.* **2** 211–22

Tuulonen A and Airaksinen P J 1996 Polarimetry of the retinal nerve fibre layer *Current Opinion in Ophthalmol.* **7** 34–8

Van de Velde F J, Jalkh A E, Katsumi O, Hirose T, Timberlake G T and Schepens C L 1990 Clinical scanning laser ophthalmoscope applications: an overview *Scanning Laser Ophthalmoscopy and Tomography* ed J E

Nasemann and R O W Burk (Munich: Quintessenz) pp 35–48

Van Norren D and Van De Kraats J 1989 Imaging retinal densitometry with a confocal scanning laser ophthalmoscope *Vision Res.* **29** 1825–30

von Ruckmann A, Fitzke F W and Bird A C 1995 Distribution of fundus autofluorescence with a scanning laser ophthalmoscope *Br. J. Ophthalmol.* **79** 407–12

Webb R H 1990 Scanning laser ophthalmoscope *Noninvasive Diagnostic Technique in Ophthalmology* ed B R Masters (New York: Springer) pp 438–50

Webb R H and Delori F C 1988 Multispectral imaging reflectometry with the confocal scanning laser ophthalmoscope *Invest. Ophthalmol. Vis. Sci.* **29** (ARVO Suppl) 339

Webb R H, Hughes G W and Delori F C 1987 Confocal scanning laser ophthalmoscope *Appl. Opt.* **26** 1492–9

Webb R H, Hughes G W and Pomerantzeff O 1980 Flying spot TV ophthalmoscope *Appl. Opt.* **19** 2991–7

Weinreb R N, Lusky M, Bartsch D U and Morsman D 1993 Effect of repetitive imaging on topographic measurements of the optic nerve head *Arch. Ophthalmol.* **111** 636–8

Weinreb R N, Shakiba S and Zangwill L 1995 Scanning laser polarimetry to measure the nerve fiber layer of normal and glaucomatous eyes *Am. J. Ophthalmol.* **119** 627–36

Wolf S, Arend O and Reim M 1994 Measurement of retinal haemodynamics with scanning laser ophthalmoscopy: reference values and variation *Surv. Ophthalmol.* **38** S95–100

Wolf S, Arend O, Sponsel W E, Schulte K, Cantor L B and Reim M 1993 Retinal haemodynamics using scanning laser ophthalmoscopy and hemorheology in chronic open-angle glaucoma *Ophthalmology* **100** 1561–6

Wolf S, Arend O, Toonen H, Bertram B, Jung F, and Reim M 1991 Retinal capillary blood flow measurement with a scanning laser ophthalmoscope. Preliminary results *Ophthalmology* **98** 996–1000

Wolf S, Toonen H, Koyama T, Meyer-Ebrecht D and Reim M 1990 Scanning laser ophthalmoscopy for the quantification of retinal blood-flow parameters: a new technique *Scanning Laser Ophthalmoscopy and Tomography* ed J E Nasemann and R O W Burk (Munich: Quintessenz) pp 91–6

Woon W H, Fitzke F W, Bird A C and Marshall J 1992 Confocal imaging of the fundus using a scanning laser ophthalmoscope *Br. J. Ophthalmol.* **76** 470–4

Woon W H, Fitzke F W, Chester G H, Greenwood D G and Marshall J 1990 The scanning laser ophthalmoscope. Basic principles and applications *J. Ophthalm. Photogr.* **12** 17–23

Wynn-Williams G M and Crowe W E 1986 Laser scanning: a method of retinal imaging *Aust. Phys. Eng. Sci. Med.* **9** 153–62